JOURNAL OF PROPULSION AND POWER
Vol. 14, No. 6, November–December 1998

Ignition and Combustion of Aluminum Particles in $H_2/O_2/N_2$ Combustion Products

Robert O. Foelsche,* Rodney L. Burton,† and Herman Krier‡
University of Illinois at Urbana–Champaign, Urbana, Illinois 61801

The ignition and combustion of aluminum particles is studied at high pressures and temperature in the combustion products of nitrogen-diluted premixed H_2/O_2 mixtures in a high-pressure, constant-volume combustion chamber. A novel approach is used to inject particles after sufficient delay for gas-phase combustion transients to equilibrate, permitting the particles to ignite and burn at high ambient temperature and nearly constant pressure conditions. Particle ignition and combustion are monitored optically by measuring combusting particle emissions. The methodology is used to measure the ignition and combustion times of ~22-μm spherodized aluminum particles over a range of pressures (38–145 atm), at 2630 K, and in 20% excess oxygen concentration. Measured ignition delays and combustion times are compared to independent data showing very good agreement.

Introduction

IN this study aluminum (Al) particle ignition and combustion are investigated at high temperatures and pressures that are formed by the spark-initiated combustion of N_2-diluted premixed H_2/O_2 mixtures in a constant-volume combustion chamber. This technique is suitable for very high-pressure combustion studies in that final pressure is only limited by the fill pressure and strength of the pressure vessel; a 6- to 8-fold increase in pressure is easily achieved without reliance on detonations or shocks. Unlike a shock-initiated particle ignition technique however, where the rise in ambient pressure and temperature is on the order of a microsecond, in the combustion chamber the establishment of quasisteady conditions takes several milliseconds. Consequently, to avoid particle combustion during gas-phase ignition transients, a novel particle injection technique has been developed where particles are injected into the hot ambient gases after a sufficient time delay. Details of the facility and its capabilities may be found in Refs. 1 and 2.

Experimental Description

The combustion chamber is a high-pressure, constant-volume combustion bomb designed for transient pressures up to 3400 atm and transient peak temperatures to 4000 K for 1-MJ energy release. The vessel shown schematically in Fig. 1a measures 66 cm tall by 51 cm diameter and is capped by a 25-cm-diam top plug that closes the central 2.0-l cylindrical chamber cavity, where the combustion chamber cavity has a diameter of 14 cm. Diagnostic access includes transient pressure measurement with a recess-mounted PCB Piezotronics, Inc. model 109 A piezocrystal pressure transducer, optical emission collection through a centerline viewing high-pressure optical window, and transferal to narrow bandpass-filtered photodiode detectors through a six-core fiber-optic cable, injection timing measurement, and spark ignition by foil-type igniter (which precludes precise gap sizing at various pressures). The constituents of a combustible mixture are successively metered into the chamber over a 20-min interval and allowed to mix for an additional 10 min, after which the mixture is ignited by a spark discharge. Initial constituents were deemed to be well mixed because it was shown that an additional 30 min mixing produced no observable change in combustion pressure rise and hot-gas emissions.

To study particle ignition and combustion dynamics at well-defined conditions, particle injection is delayed. The delayed injection sequence is shown schematically in Fig. 1b. The figure shows two cross sections of the central chamber cavity, where the first instant is prior to particle injection, during which time the particles are not exposed to the hot gases and rapidly changing pressure conditions. The pressure rise in the chamber because of gaseous mixture combustion drives a tiny piston to inject particles, as shown in the second half of Fig. 1b. This device has been described in detail elsewhere[1,2] and provides good particle dispersion at high gas densities with an initial injection velocity of ~12 m/s. The particles are injected into the hot and slowly decaying pressure gases, where they ignite and burn to completion within the conical field-of-view of the optical window and fiber optic.

A measured pressure signal from a typical experimental condition is shown in Fig. 2. In the figure spark ignition of the initial gas mixture occurs, followed approximately 0.5 ms later by the pressure rising in the combusting mixture, reaching a peak, and then decaying slowly. Pressure rise times (t_{pr}) for the gas mixture used in the experiments are 1.2 ± 0.3 ms at ~145 atm, decreasing slightly to 1.0 ± 0.1 ms at 37.5 atm, where t_{pr} is taken to be the time between 10 and 90% of the measured pressure rise. The total test time or stay time (t_{ps}) is determined by the degree of pressure falloff that is deemed acceptable. The oscillation in the pressure signal is not well understood but is most likely the radial ringing of the metal chamber. An approximate calculation of the radial "breathing" oscillation of the chamber gives a frequency of 3.2 kHz, which would not die out rapidly. The measured frequency is 3.90 ± 0.10 kHz and is very repeatable between experiments and does not decay for the ~30 ms over which data are taken. The estimated longitudinal frequency would be less than 1 kHz, and the noise is not believed to be pressure oscillations in the gas phase because the frequency is independent of initial chamber pressure and mixture stoichiometry for those mixtures where the ringing occurs.

Received Nov. 20, 1997; revision received April 9, 1998; accepted for publication April 10, 1998.

*Ph.D., Department of Aeronautical and Astronautical Engineering; currently Scientist, GASL, Inc., 77 Raynor Avenue, Ronkonkoma, NY 11779. Student Member AIAA.

†Professor, Department of Aeronautical and Astronautical Engineering. Associate Fellow AIAA.

‡Professor, Department of Mechanical and Industrial Engineering. Fellow AIAA.

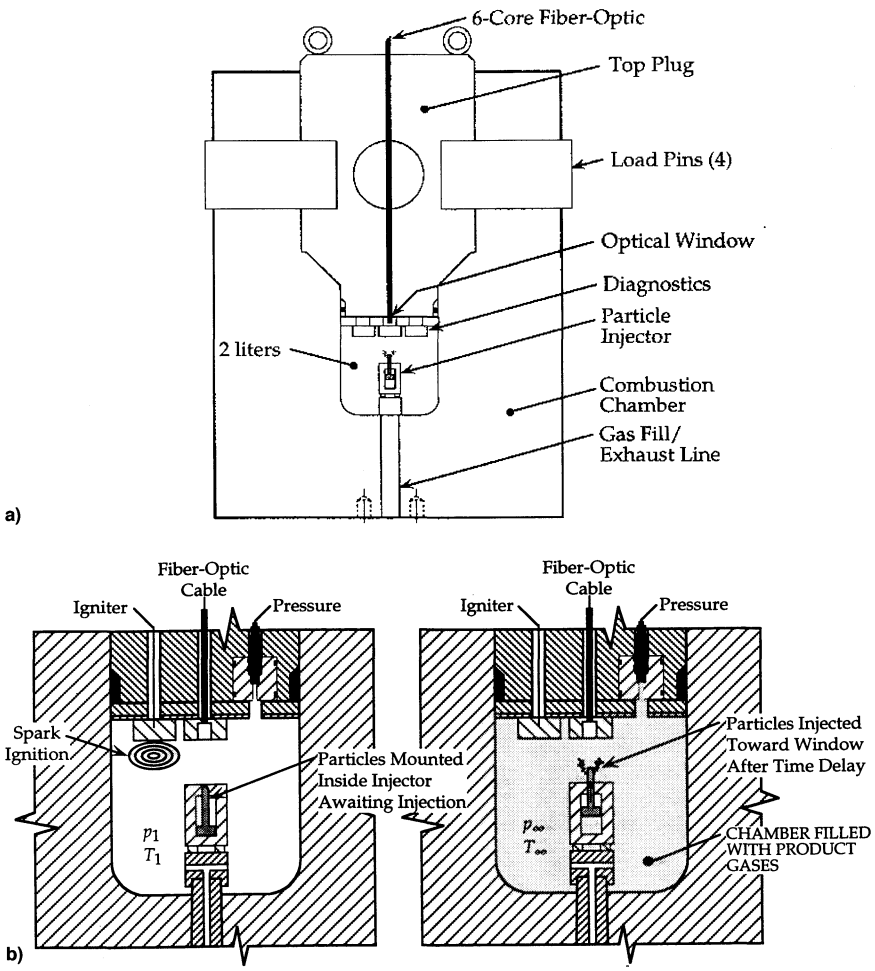

Fig. 1 Schematic of a) high-pressure combustion chamber with a 2.0-l central cavity and b) delayed particle injection sequence.

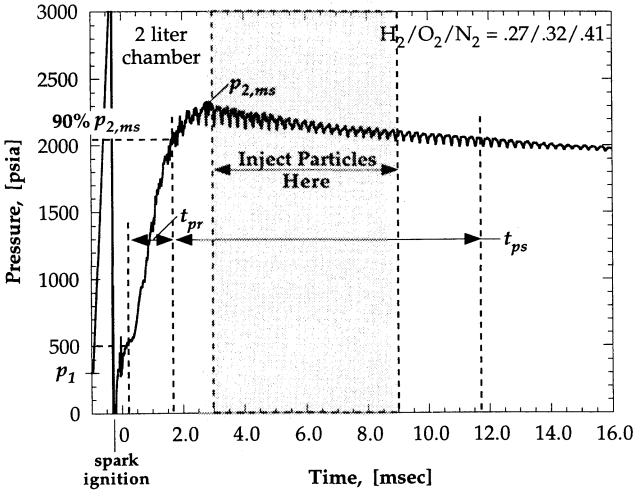

Fig. 2 Typical pressure signal in combustion chamber shows a rise to peak pressure on a millisecond time scale, after which time particles are introduced.

Gas Mixture Combustion and Pressure Decay

Mixtures of N_2-diluted premixed H_2 and O_2 are combusted to provide various high-temperature, high-pressure mixtures of prescribed gas composition for conducting particle combustion experiments. The fuel and oxidizer choice provides rapid combustion, simple products, and high temperatures. (N_2 is a convenient detonation preventer and is furthermore used to control test temperatures while providing similar mixture properties to air.) The initial mixture used is listed in Table 1 (referred to as state 1) along with gas-phase products predicted by an equilibrium code,[3,4] (referred to as state 2). Product mole fractions are assumed to remain fixed at their initial equilibrium values throughout particle lifetimes, even though the pressure and temperature decay slowly (p_∞ and T_∞), this assumption being most valid for stable compounds (N_2, H_2O, and O_2) and within 5% for gas-phase radicals. Only a single mixture at three differing initial pressures (5.8, 10.4, and 20.4 atm) was used in studying Al particle ignition delays and combustion times. This mixture is a subset of those used in a broader study of boron (B) particle ignition and combustion over a range of pressures, temperatures, excess oxygen, and ignition-enhancing additives.[1,2] The mixtures tested were found to be nondetonable in the given combustion vessel geometry.

It is desirable to retain a fairly constant pressure over the particle ignition and combustion lifetime to determine particle ignition and combustion times at a known pressure. Because chamber pressures decay slowly with time (Fig. 2), particle combustion does not occur at a constant pressure, but at a nearly constant pressure. The pressure stay time, defined as the time over which the pressure does not change more than ±5%, is approximately 11 ms at ~145 atm and 7 ms at 37.5 atm. In general, for these Al particle tests, however, the pressure (and temperature) drop is less than 5%, being ~2 atm (1.4%) at high pressure and ~1 atm (2.8%) at low pressure.

After peak pressure is reached within ~1.5 ms of H_2/O_2 gas ignition, the chamber pressure is seen to decay slowly at a rate of ~0.2%/ms. This is likely a result of gas heat losses, where the possible heat loss mechanisms include conduction, radiation, and water-vapor condensation on the surrounding metal chamber walls. Simple transient one-dimensional conduction heat transfer analysis[5] for a hot sphere of gas conducting to a

Table 1 Premixed N_2-diluted H_2/O_2 mixtures[a]

Initial mix mole fractions				Final mix mole fractions						
p_1, atm	H_2	O_2	N_2	p_2, atm	T_2, K	O_2	H_2O	N_2	NO	OH
5.8	0.28	0.32	0.40	46	2725	0.19	0.31	0.45	0.02	0.02
10.9	0.27	0.32	0.41	84	2665	0.20	0.30	0.45	0.02	0.01
20.4	0.27	0.32	0.41	158	2675	0.20	0.30	0.45	0.02	0.01

[a]Used for establishing high pressure and temperature conditions for particle combustion. Combusted product mixture mole fractions and conditions are predicted with an equilibrium code.

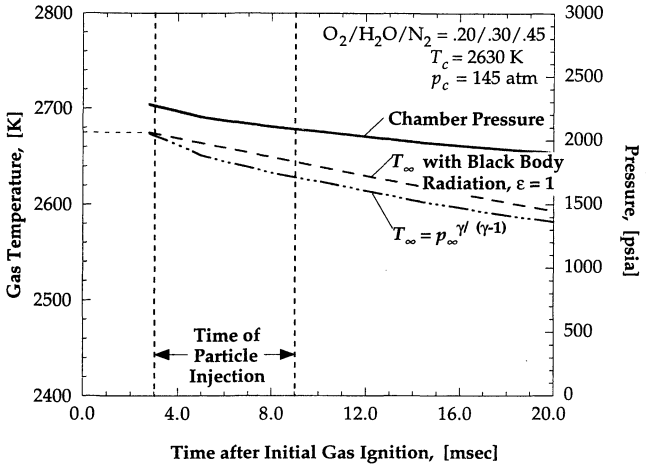

Fig. 3 Calculated ambient gas temperature falloff at 145 atm based on measured pressure decay compared to radiation loss from a sphere of zero optical depth.

cold wall at constant temperature (because the wall thermal conductivity $k_w >> k_g$ the gas thermal conductivity) gives a characteristic conduction heat-loss time constant for gases at the center of the chamber between 30 and 80 s for the gas mixture at 37.5 and 145 atm. The corresponding characteristic radiation heat-loss time constants, assuming the gas volume radiates as a blackbody with zero optical depth corresponding to the greatest heat-loss case possible, are 0.9 and 3.3 s, respectively. These numbers indicate that heat losses at the center of the chamber, where particles are injected, occur on long time scales compared with the particle ignition and combustion times that are on millisecond time scales.

However, heat losses are not negligible at the periphery of the vessel. At high pressure the total chemical energy release is ~110 kJ for the mixture employed to study Al particle combustion. The heat transfer analysis for a conducting sphere predicts a heat loss of approximately ~16 J/ms and heat transfer from a sphere radiating as a blackbody ($\varepsilon = 1$) is ~750 J/ms, so that the fractional loss per ms is 0.7% of the total energy. In the ~20 ms time frame for particles to be injected, ignited, and burned to completion, the energy lost will therefore be small compared to the gas total energy. This energy-loss rate is compared with the measured pressure decay for the same mixture that is 1.1%/ms. These rough calculations suggest that the pressure drop in the chamber can be accounted for by gas heat losses at the walls of the chamber. Condensation losses in the growing thermal layers along the chamber walls are confined to a region less than ~0.2 mm thick during the time frame of particle injection and combustion, resulting in a fractional mass loss less than ~0.1% from the 30% water-vapor gas mixture, which is negligible.

Based on the long characteristic heat-loss time scales for conduction and radiation at the center of the chamber, but non-negligible losses near the walls, it is assumed that gases at the center of the chamber where particles are injected are expanding adiabatically and ambient temperatures $T_\infty(t)$ are calculated from the measured pressure decay by $p_\infty/T_\infty\gamma/(\gamma^{-1}) = \text{const}$. With this assumption the differential temperature loss rate for the mixture at high pressure is $\Delta T_\infty/T_\infty = 0.2\%/\text{ms}$. The resulting temperature decay rate for most mixtures is ~5 K/ms.

The theoretically calculated temperature decays from heat losses are shown in Fig. 3 and are compared to temperatures calculated assuming an adiabatic process at the center of the chamber. It is seen that the agreement at high pressure (145 atm) is very good, within 20 K, and except for the initial 3–4 ms, the heat-loss rate also agrees very well. At a lower pressure (37.5 atm) the temperatures calculated from measured pressures decrease much less rapidly than radiation losses predict ($\varepsilon = 1$), indicating that the gases are likely not radiating as strongly as assumed (best agreement for $\varepsilon = 0.5$, not shown in Fig. 3).[1]

Description of Aluminum Powder

Several tests were conducted with spherodized Al particles identical to those used previously by Roberts et al.[6,7] All powder samples were received containing particles ranging from submicron to approximately 100 μm in diameter, and were subsequently sieved into tighter-size distributions to produce experimental results tenable to meaningful analysis. Characteristics of the various samples are given in Table 2 and were obtained from Valimet, Inc. Samples were separated by micromesh sieving and classified under a scanning electron microscope (SEM).

Photomicrographs were taken with an ISI-DS130 and Hitachi S-800 SEM at various magnifications. Size distributions were measured manually by counting 100–200 randomly chosen particles on the SEM photograph. Photomicrographs were scanned into a computer and two perpendicular dimensions recorded with the use of fine-measurement grids, with the dimensional error being approximately ± 0.5 μm. In each case two dimensions were recorded along with the approximate shape of the particle; either a sphere or prolate spheroid.

Figure 4 shows a photomicrograph and particle-size histogram of one of the Al particle samples used. Photomicrographs of the Al show that the particles are uniform and spheroidally shaped. The 20–25 μm sample shows very uniform particles with an effective mean diameter of 21.6 $\pm$ 2.4 μm and the larger particle sample has an effective mean diameter of 53.1 $\pm$ 5.2 μm, but most of these particles are oblong and characterized as prolate spheroids.

Optical Emission Detection

Particle combustion time histories are measured indirectly by monitoring combustion emissions at selected wavelengths to filter out as much of the hot ambient gas radiation as possible. An optical narrow bandpass filter is used to monitor emissions centered on the AlO(g) molecular band at 485 nm (filter 486.1 $\pm$ 4 nm, Ealing Electro-Optics, Inc.). The AlO(g) molecule is a reactive intermediary gas-phase species formed during Al particle combustion that gets oxidized further into $Al_2O_3(s)$. Little dissociated Al_2O_3 is expected at the temperatures investigated; therefore, once the source of Al is consumed so is the source of AlO(g).

The AlO spectrum is readily observable during the combustion stage and the choice of bands is based on analysis of spectra obtained with a gateable optical multichannel analyzer.[8] A typical combusting Al particle spectrum consists of the hot particle broadband contribution onto which the readily

Table 2 Characteristics of the aluminum powder samples used in the combustion experiments[a]

Particles	Form	Mesh size	Effective diameter, μm: Mean	Median	Standard development	Supplier
Al	Spherodized	20–25	21.6	21.7	2.4	Valimet, Inc.
Al	Spherodized	45–53	53.1	52.3	5.2	Valimet, Inc.

[a]References 1 and 3.

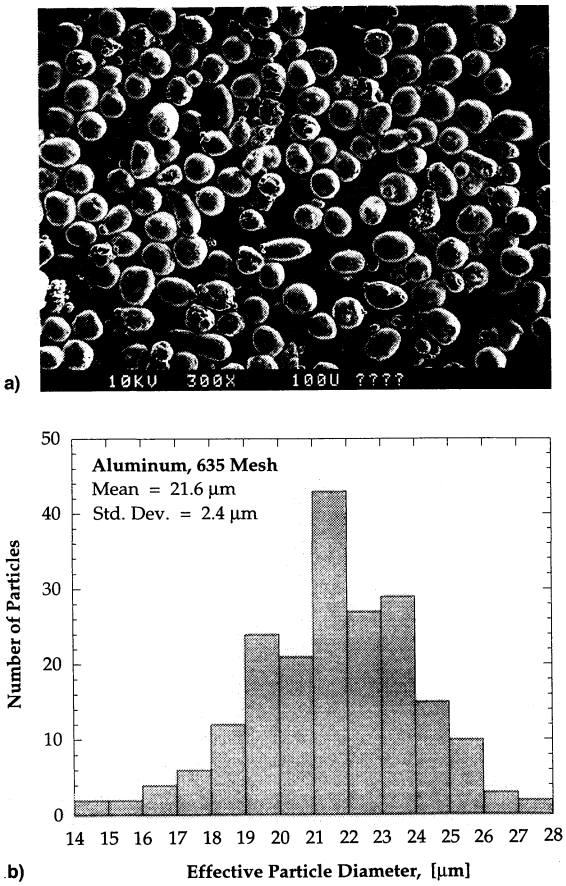

Fig. 4 a) Photomicrograph at 300× magnification and b) particle size distribution of 20–25 μm aluminum powder from Roberts.[6]

identifiable AlO spectrum is superposed. Thus, optical filtering about AlO bands, where the signal is composed of both hot particle and AlO(g) emissions, is considered a good indication of both particle ignition (thermal runaway) and combustion. It is noted that during the end stages of combustion, when a hot Al droplet becomes vanishingly small and AlO is converted to products, condensed Al_2O_3 smoke emissions may lead to interference with the measured signal.[9,10]

Interpretation of Measurements

Typical Al particle combustion measurements are shown in Figs. 5 and 6. Both signals have been smoothed to remove noise greater than 100 kHz. Figure 5 shows an Al particle measurement and hot-gas background (no particles are present) measurement at identical ambient conditions of Fig. 2. It is seen that after spark ignition, the pressure and hot-gas emissions rise to peak levels. Then at 4.1-ms Al particles are injected as indicated by the injection-timing mark in Fig. 5 (from a make-switch device that is an integral part of the injector). Shortly after injection the bandpass-filtered photodiode measurement centered at 486.1 nm shows a rapid increase in luminosity above the background level because of particle ignition. This is followed by a peak in the particle signal and an eventual return of measured luminosity to the background gas-

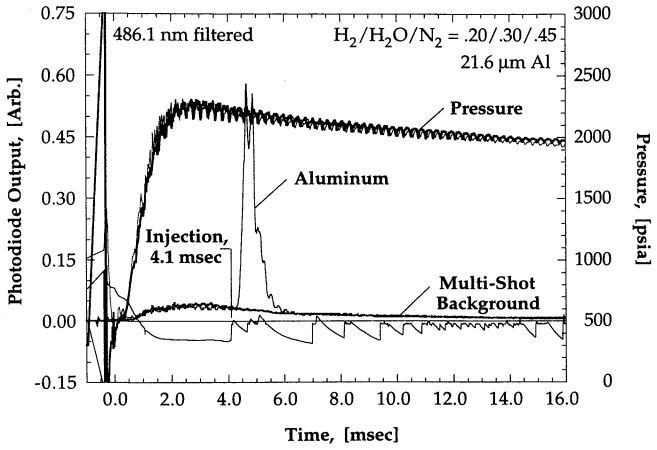

Fig. 5 Typical 486.1-nm filtered Al particle emission signal for particles combusting in gas mixture of Fig. 2. Particles are injected at 4.1 ms.

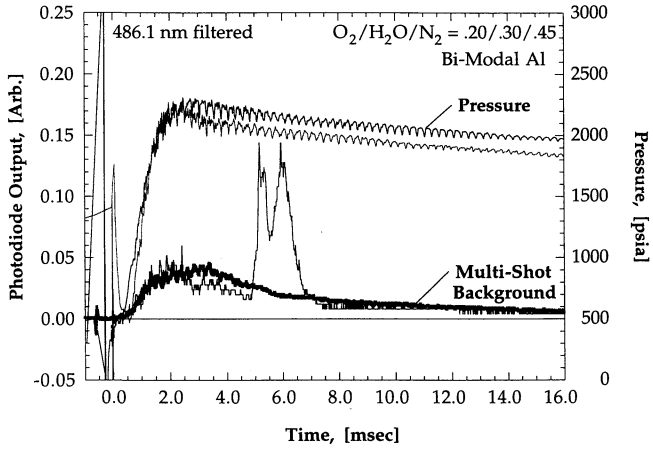

Fig. 6 Typical net particle signal for Al powder with bimodal size distribution, ~22 μm plus ~53 μm, showing two resolved peaks.

emission level, indicating that particle combustion and conversion to gas-phase products is complete. The measured particle emissions tend to linger for a short time on approach to background levels, producing what resembles a tail on the particle trace. In Fig. 5 the filtered emissions of the hot background gases are negligible compared to the Al particle emissions. In Fig. 6 two distinct peaks are measured when a mixture of two particle sizes is injected, where the individual constituents ignite and burn to completion independent of the other, as will be discussed later.

The chamber pressure is unaffected by particle combustion. Similarly, the bulk gas mixture composition is unaffected for extended periods of time as seen by the excellent match between particle-laden and background hot-gas emissions after particle combustion is completed. For all tests conducted, the mass of Al particles introduced is negligible compared to the bulk gas mass, ~1:12500 for the lowest pressures studied (37.5 atm). The Al particle sample that provides sufficient dis-

tinguishable signal strength is approximately 10% (by the number of particles) of the corresponding B sample used in Ref. 1, this being a result of Al burning much more brightly than B at the conditions tested.

Definitions of Ignition Delay and Combustion Times

Ignition delays and combustion times are determined from the time-resolved filtered photodiode measurements. A net-particle emission trace is first produced by subtracting a multishot composite background signal from each particle-laden measurement. Ignition is defined as occurring at the half-maximum point in the net-filtered photodiode signal, and ignition delay time is then from the time the temperature stimulus occurs, when particles are injected, up to the point of ignition. Combustion times are determined by two methods that are compared in this paper. The first method defines combustion time as the time from ignition to the time when the net-filtered signal has fallen back to half-maximum.[1,2,7,11] The second method defines combustion time as lasting up to the point where 90% of the area under the net-filtered signal is reached.

The experiments conducted are not single-particle experiments, but instead use large numbers of particles to obtain discernible particle emission levels. These particles are shown to disperse well upon injection and to ignite and burn to completion independently of each other. The particles used have discernible variations in size and also in shape, although the majority are spheroids (Fig. 4a). However, these factors are mitigated by defining combustion time in a statistical sense to indicate when the majority of the particles are consumed, by using the time between the half-maxima similar to studies by Roberts et al.[6,7] and Megli et al.[11,12] Multiparticle tests, where the overall mass is still small, ~0.8 mg, alleviates the problems arising from individual particle variations by introducing statistical averaging.

The second definition for combustion times correlates the total area under the net-particle signal to the amount of energy released in a certain spectral bandwidth.[9] Then the particles are considered to be approximately burned to completion when the majority of their useful energy has been consumed as determined by their luminous brightness, where the remaining luminosity is considered as either negligible energy release or possibly as lingering emissions from the hot oxides that are formed. In this study a value of 90% of the total area under the net-particle signal curve is chosen as the point when particles burn to completion according to this definition. The combustion time, $t_{c:90}$, is then defined as lasting from the point of ignition, still defined by the half-peak amplitude method, to the time when the 90% area is reached. By stipulating combustion to occur when too large a percentage of the total area under the emission curve is attained, the burn times of the largest effective diameter particles are being measured including interferences from the glow of lingering embers or smoke emissions, e.g., $Al_2O_3(s)$.

Al particle lifetimes for the particles under study are short enough to treat the bulk gas properties as nearly constant. As such, the time-averaged pressure and temperature during each stage is treated as a constant and the falloff is ascribed to the uncertainty. Error bars given in Figs. 7 and 8 for p_c and p_b are defined as $\pm\sigma$ (standard deviation), plus the instrument sensitivity and uncertainty from finite A/D discretization, the sum of which may be too small to appear clearly in the figures. Uncertainties in quoted temperatures are predominantly from uncertainties in the measured initial mixture composition, which although being small, have a larger effect on equilibrium-predicted combustion temperatures. The overall uncertainty in quoted T_c is ±40 K at ~145 atm and ±80 K at 37.5 atm.

Uncertainties in measured t_{ign} and t_c are a result of the net particle signals' interpretation. Contributing to these uncertainties are multiple peaks in the collected particle-emission signals, which affect determination of peak and half-peak amplitudes, uncertainty in the average no-particle signal, and uncertainty caused by any oscillations in the tail of the emission trace. These uncertainties are generally small, ~10 μs, compared to the injection timing uncertainty caused by the finite time to inject the entire particle sample, which is generally ±60 μs.

Experimental Results

Measurement of Particle Ignition Delays

The high-pressure ignition delay and combustion time measurements obtained for Al with conditions listed in Table 3 are plotted in Figs. 7 and 8, and show that Al ignition delays decrease by a factor of ~2 as pressure is increased from 37.5 to 140 atm in a mixture of O_2/H_2O = 0.20/0.30 at ~2630 K, with the balance N_2. The measured pressure dependence can be fit by a function of the form given by Eq. (1), with time in milliseconds and p_c in atmospheres. Ignition times for ~22 μm particles are less than 1 ms at the conditions tested:

$$t_{ign} = 6.8p_c^{-0.6} \quad (1)$$

It is not possible to perform tests with the present injector at even lower pressures, and so these data are extrapolated to lower pressures to compare to independent measurements. The lower-pressure ignition data of Roberts et al.[7] in 100% oxygen show a definite pressure effect between 8.5 and 34 atm, and that delays increase with a decrease in temperature from 2775 to 2230 K. The data of Megli et al.[11] at 8.5 atm and 2700 K indicate that reducing the ambient oxygen to 60% in Ar increases ignition delays compared to Roberts et al.'s 100% O_2 data.[7] Roberts et al.'s[7] and Megli et al.'s[8] measurements were conducted behind reflected shocks in a 9-cm-diam test-section shock tube with identical aluminum particles as used here. The ignition delays of Belyaev et al.[13] were obtained in propellant product gases at 2800 K, but with similar pressures as measured here, using larger 70-μm particles scaled down to the size of interest using a d_p^2 dependence.

In both the shock-tube and combustion-chamber experiments convective effects play important roles during particle ignition and combustion, making it necessary to examine dif-

Table 3 Measured ignition delay and combustion times of aluminum particles as a function of pressure at ~2630 K

Shot no.	T_1, K	p_1, atm	d_p, μm	O_2	H_2O	T_c, K	p_c, atm	t_{ign}, ms	p_b, atm	t_c, ms	$p_{b:90}$, atm	$t_{c:90}$, ms
3.17	293.7	20.7	21.6	0.20	0.30	2652	149.0	0.44	147.7	0.42	147.5	0.71
3.18	301.1	20.7	21.6	0.21	0.30	2613	133.8	0.21	133.2	0.80	132.8	1.25
4.11	293.5	20.6	21.6	0.20	0.30	2617	138.5	0.40	138.2	0.36	138.1	0.53
3.30	296.0	10.9	21.6	0.21	0.30	2576	——[a]	——[a]	70.4	0.88	70.4	0.95
3.37	296.4	10.9	21.6	0.21	0.30	2597	——[a]	——[a]	70.0	0.80	69.7	2.47
3.95	294.0	5.8	21.6	0.19	0.32	2680	40.3	0.66	39.6	0.90	39.6	0.85
3.96	293.8	5.8	21.6	0.19	0.31	2647	37.8	0.78	37.2	1.13	37.2	0.91
4.21	291.1	5.8	21.6	0.19	0.31	2621	37.8	0.88	36.7	0.99	36.6	1.30
5.02	298.2	20.7	53.1	0.20	0.30	2625	145.9	1.05	144.0	0.77	142.4	2.65

[a]Ignition delays unavailable, no timing device present.

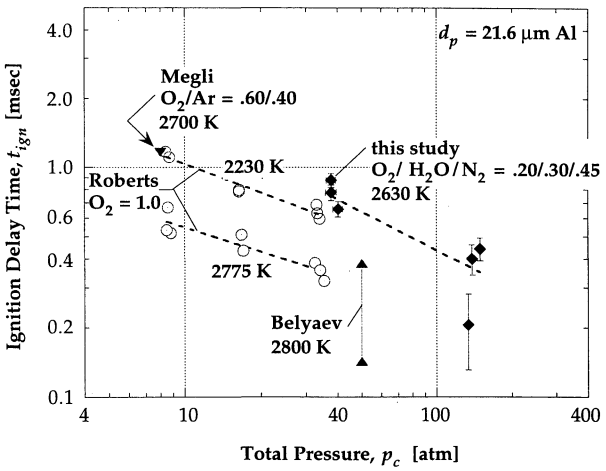

Fig. 7 Measured aluminum particle ignition delays show similar pressure dependence to data of Roberts. Reduced O_2 and lower temperatures result in longer delays as expected.

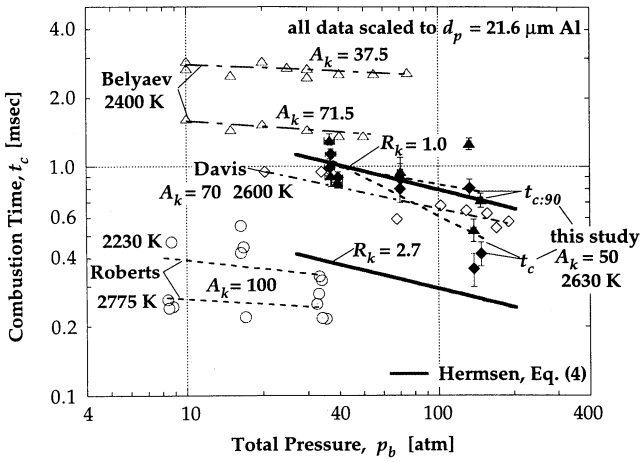

Fig. 8 Comparison of measured aluminum particle combustion times. The times t_c provide the best agreement with Davis[15] data and with empirical Hermsen formula.

ferences in these effects between the various experiments. According to Roberts,[6] time-averaged particle Nusselt numbers during ignition, where particles are accelerated by the flow behind the incident shock wave in the shock tube, are typically ~4 and typical gas thermal conductivities fall between 0.14 and 0.20 W/m K over the temperature range of interest, 2200–2800 K. The resulting convective heat transfer coefficients defined by $\bar{h}_c = Nu_p k_g/d_p$ fall in the 25–37 kW/m^2 K range, which spans the range of values for particles injected into the combustion chamber at higher pressure.[1] Here Nu_p is the particle surface-averaged Nusselt number that has been determined empirically to be a function of the particle Reynolds number (Re_p), k_g is the gas thermal conductivity, and d_p is the particle diameter. Thus, convective heating processes are similar in both experiments, permitting a direct comparison of results. When the measured trend at a high pressure, with 50% combined O_2 and H_2O at 2630 K, is extrapolated to still lower pressures, agreement is obtained with the shock-tube data of Megli et al.[11] in reduced oxygen mixtures (60% O_2 at 2700 K). The good agreement of the new data with these other independent studies leads to the conclusion that the particle injection technique is valid.

The high ambient temperatures are the driving potential behind particle ignition and subsequent self-sustained combustion. To ignite, the particles must first be heated sufficiently for their oxide coating to melt and retract on the surface, exposing the underlying Al, so that heterogeneous surface oxidation takes place, leading to rapid temperature rise and self-sustained combustion. This heating period is accelerated in the present experiments by convective effects resulting from particle injection. The convective heating rate using simple one-dimensional analyses for spherical particles[1,2] is directly proportional to a surface-averaged Nu_p, which can be expressed empirically as a function of the particle Re_p.[14] With Re_p being directly proportional to pressure (density), increased convective heat transfer rates are obtained at elevated pressures thereby increasing the ignition rate. Additionally, as the particle temperature increases and the particles melt, the base metal thermally expands more quickly than the protective oxide coating, producing cracks in the coating that provide a direct path for oxygen to react with the subsurface nascent Al prior to full ignition.[10] Higher ambient oxygen partial pressures accelerate this process through increased gas-phase transport from higher concentration gradients.

Measurement of Particle Combustion Times

Combustion times defined by the times at half of peak amplitude are compared to similar high-pressure data in Fig. 8 and show good agreement with other determinations. The data from the present experiments can be fit as a function of pressure by

$$t_c = 7.5 p_b^{-0.55} \tag{2}$$

These new data are compared to the Al particle data of Davis,[15] who measured particle luminosity tracks in a closed bomb charged with N_2, where pellets of propellant and oxidizer containing low loadings of Al particles were ignited and burned, and Belyaev et al.,[13] who used similar techniques but in a half-closed bomb where the particles burned in a high-temperature gas flow. These previous studies examined much larger particles between 53 and 140 μm than were used in the present study, but particle-size-scaling relationships were determined in each case. The large particle data of Davis and Belyaev et al. have been scaled to a diameter of 21.6 μm using the respectively determined scaling relationships, $t_c \sim d_p^{1.8}$ (Davis), and $t_c \sim d_p^{1.5}$ (Belyaev et al.), to compare with data obtained in the shock tube[7,11] and combustion chamber. The data of this study compare most closely with Davis et al.'s determination, but show a greater pressure dependency than all other measurements.

The nature of the convective environments in the Davis and Belyaev et al. experiments is not known, but it is important even in an enclosed bomb where the burning propellant gases evolve from the propellant surface at a nonnegligible velocity exceeding the particle velocity. However, the nature of the relative slip flows in the shock-tube experiments of Roberts et al.[7] and Megli et al.[11] are known. For average particle velocities of ~10 m/s during combustion in the reflected shock region, typical $Re_p \approx 4$–8 (where Re_p is the particle Reynolds number based on the particle diameter d_p), which are again typical of conditions in the high-pressure experiments of this study. During combustion the convective heating (or cooling) is not as important as the deformation of the reaction zone and product cloud surrounding the burning Al droplet. Al generally burns in the vapor phase and transport of oxidizers and products to and away from the surface are accelerated by convective flow around the particles.

Various other Al particle combustion data have been determined over a range of pressures, particle sizes, and differing oxidizing atmospheres. Hermsen proposed an empirical relationship to calculate combustion times in terms of these parameters for various oxidizing atmospheres

$$d_p^{1.8} = d_{p,0}^{1.8} - \beta t \tag{3}$$

where β is the combustion rate.[16] The combustion time can be found by setting $d_p \approx 0$, giving

$$t_c = d_{p,0}^{1.8}/\beta \tag{4}$$

where $\beta = 8.33 \times 10^{-5} R_k A_k^{0.9} p_c^{0.27}$ cm$^{1.8}$/s; R_k = 1–2.7, a parameter; and $A_k = (X_{O_2} + X_{H_2O} + X_{CO_2} + X_{O_x}) \times 100\%$, the mole fraction oxidizer, in percent p_c = gas pressure (psia) and $d_{p,0}$ = the initial particle diameter (cm).

The combustion time determined by Eq. (4) has units of seconds. The factor R_k is an empirically determined parameter to account for differences between the gas environments that typically exist in the laboratory and those in operating rocket chambers. For nonconvective, low blackbody temperature environments typical of laboratory experiments, a value of R_k = 1 is suggested. For the convective, high-blackbody temperature environments of rocket chambers, the appropriate value of 2.7 is to be employed.[16] Equation (4) is plotted along with the various data in Fig. 8. For the conditions of our mixture (Table 1), A_k = 50%, p_b = 37.5–145 atm, and for $d_{p,0}$ = 21.6 μm, the upper and lower bounds on the calculated combustion times are 660 and 245 μs, respectively, compared to 530 μs from the measurements. The new high-pressure data agree more closely with the R_k = 1 value and are found to lie between the limits calculated with the empirical relation.

Combustion times evaluated at the time corresponding to 90% of the total area are compared to Davis's measurement[15] in Fig. 8 for 21.6-μm Al particles and show a much closer agreement than values determined using the times between half of peak amplitude. The pressure dependency in $t_{c:90}$ is reduced and falls in line with the other determinations and also Hermsen's[16] empirical relation, Eq. (4); the data can be fit by

$$t_{c:90} = 2.2 p_b^{-0.21} \tag{5}$$

For Al particles the difference between t_c and $t_{c:90}$ are fairly small in an absolute sense, but not in on a relative scale because the measured times are so short. Thus, it appears that $t_{c:90}$ agree more closely with the combustion times determined in propellant product gases, which were measured up to the instant when luminous particle streaks on photographic film disappeared, even though half of the peak amplitude formalizm used here is the same as that used by Roberts et al.[7] in the shock tube. Using 100% of the total area to stipulate completed combustion results in significantly longer times that do not follow established trends in the literature. This suggests that lingering emissions from the condensed oxide cloud hampers interpretations of optical signals in the present tests as occurs at low pressures.

The agreement between the new high-pressure data and measured trends of Roberts et al.[7] and Davis[15] and the empirical formulation of Hermsen provides further evidence that the particle injection technique and interpretation of measurements is valid. The 40% drop in measured t_c is not in line with the pressure dependence displayed in other data, but $t_{c:90}$ is in general agreement with these other measurements and with Hermsen's empirical correlation. This drop in combustion times is to be expected because increased pressures lead to higher convection and transport gradients. Based on these results with Al particles a broader study of B particle ignition and combustion was undertaken, as B has received increased attention in recent years for possible application with fluorinated propellants.[1,2]

Ignition and Combustion of a Bimodal Particle Mixture

To investigate whether group particle interactions occur at high pressure and temperature, particle ignition was studied with an Al powder sample containing a bimodal size distribution. Figure 6 shows the results of injecting a mixture of ~22- and ~53-μm particles at 140 atm. The photodiode signal in Fig. 6 displays two distinct peaks associated with the two distinct particle sizes, as would be expected for particles that ignite and burn independently of one another. The particle sizes in the bimodal mixture were chosen so that the particle lifetime of the smaller constituent is shorter than the ignition delay of the larger constituent, and this is observed by the prominent valley separating the two peaks.

The measured ignition delay and combustion times corresponding to the first peak in Fig. 6 give $t_{ign}^{(1)}$ = 430 ± 70 μs and $t_c^{(1)}$ = 450 ± 75 μs, whereas for the second peak $t_{ign}^{(2)}$ = 970 ± 120 μs and $t_c^{(2)}$ = 740 ± 125 μs. The times for the first peak that can be attributed to the smaller particles agree well with the data obtained separately for ~22-μm particles, t_{ign} = 350 ± 130 μs and t_c = 530 ± 240 μs. The ignition delay and combustion times for the second peak are in agreement with a single measurement for ~53-μm particles tested separately, t_{ign} = 1050 ± 80 μs and t_c = 770 ± 145 μs. The measurements shown in Fig. 6 with the bimodal powders confirm that particles injected into the chamber at high pressure do in fact ignite and burn independently of one another. It is noted that ignition delays scale less strongly than a d_p-squared dependence expected for particles heating under stagnant conditions (no relative motion), indicating that delays are shortened significantly by convective heating.

Summary

An experiment has been designed and developed that permits small particle ignition and combustion studies to be conducted in gaseous mixtures at high pressures and high temperatures produced by the combustion of gaseous fuel/oxidizer mixtures. In this study N_2-diluted premixed H_2/O_2 mixtures were used. Once a combustible mixture is ignited and peak pressure is reached, the pressure in the experimental chamber decays slowly, permitting particle tests to be conducted at nearly constant pressure and temperature conditions. Using a novel particle injector, Al particles are introduced rapidly after a sufficient time delay so that they may ignite in short time scales and burn to completion independently of one another. Analysis indicates that the injected particles experience increased heating rates during the ignition stage resulting from their motion through the dense gases. Particle ignition and combustion are monitored by measuring emissions with fast-response photodiodes using narrow bandpass filters. The experimental approach was validated by various means and calibration against the independent measurements shows good agreement for Al particle ignition delays and combustion times.

When the measured ignition delay trend at high pressures, with 50% combined O_2 and H_2O at ~2630 K, is extrapolated to still lower pressures, agreement is obtained with the shock-tube data of Megli et al.[11] in reduced O_2 mixtures (60% O_2 at 2700 K). Similar agreement is shown between newly measured combustion times and data of Davis[15] in propellant product gases. The good agreement of the new data with these other independent studies, and the particle dispersion test with bimodal particle mixtures, leads to the conclusion that the particle injection technique produces valid single-particle data and that the correlations of Hermsen for Al combustion are indeed valid.

Acknowledgments

This work was sponsored by the Office of Naval Research under ONR Grant N00014-93-1-0654. Richard S. Miller was the Project Director. The authors are indebted to the Department of Aeronautical and Astronautical Engineering at the University of Illinois for its support and facilities, and to P. Hetman for his expert fabrication and machining of the combustion chamber and special insights into the main seal design. Acknowledgment also goes to D. Roberts, R. Hendricks, and R. Coverdill of the Mechanical Engineering Shop for their expert work during the fabrication of related assemblies, C. Reiner for the design and fabrication of specialized electronics, and D. Schneider and M. Abogado for assistance with execution of the experiments.

References

[1]Foelsche, R. O., "Ignition and Combustion of Boron Particles in Hydrogen/Oxygen Combustion Products at 30 to 150 Atmospheres, Ph.D. Dissertation, Dept. of Aeronautical and Astronautical Engineering, Univ. of Illinois at Urbana–Champaign, Urbana, IL, 1998.

[2]Foelsche, R. O., Burton, R. L., and Krier, H., "Boron Particle Ignition and Combustion at 30–150 Atmospheres," *Combustion and Flame* (to be published) (Paper CF 97-085).

[3]Reynolds, W. C., *Stanjan-III Equilibrium Program*, Vol. 3.95, Stanford Univ., Stanford, CA, Sept. 1993.

[4]Kee, R. J., Rupley, F. M., and Miller, J. A., "The Chemkin Thermodynamic Data Base," Sandia National Labs., Rept. SAND87-8215B, Livermore, CA, 1990.

[5]Luikov, A. V., *Analytical Heat Diffusion Theory,* Academic, New York, 1968.

[6]Roberts, T. A., "The Shock Tube Ignition and Combustion of Aluminum/Magnesium Alloy Particles in Oxygen at High Pressure," Ph.D. Dissertation, Dept. of Aeronautical and Astronautical Engineering, Univ. of Illinois at Urbana–Champaign, Urbana, IL, 1993.

[7]Roberts, T. A., Burton, R. L., and Krier, H., "Ignition and Combustion of Aluminum/Magnesium Alloy Particles in O_2 at High Pressures," *Combustion and Flame*, Vol. 92, 1993, pp. 125–143.

[8]Pearse, R. W. B., and Gaydon, A. G., *The Identification of Molecular Spectra*, 4th ed., Chapman and Hall, London, 1976.

[9]Olsen, S. E., and Beckstead, M. W., "Burn Time Measurements of Single Aluminum Particles in Steam and Carbon Dioxide Mixtures," AIAA Paper 95-2715, June 1995.

[10]Price, E. W., "Combustion of Metalized Propellants," *Fundamentals of Solid-Propellant Combustion*, edited by K. K. Kuo and M. Summerfield, Vol. 90, Progress in Aeronautics and Astronautics, AIAA, New York, 1984, pp. 479–514.

[11]Megli, T. W., Krier, H., and Burton, R. L., "Shock Tube Ignition of Aluminum/Magnesium Alloys in Water Vapor and Argon," *Proceedings of the 3rd International Conference on Experimental Heat Transfer, Fluid Mechanics, and Thermodynamics*, edited by M. D. Kelleher, R. K. Shah, K. R. Sreenivasan, and Y. Joshi, Vol. 2, Elsevier, New York, 1993, pp. 1097–1105.

[12]Megli, T. W., "Aluminum-Magnesium Particle Ignition in Shocked Mixtures of Water Vapor and Argon," M.S. Thesis, Dept. of Mechanical and Industrial Engineering, Univ. of Illinois at Urbana–Champaign, Urbana, IL, 1993.

[13]Belyaev, A. F., Frolov, Y. V., and Korotkov, A. I., "Combustion and Ignition of Finely Dispersed Aluminum," *Combustion, Explosions, and Shock Waves*, Vol. 6, No. 3, 1968, pp. 182–185.

[14]Fox, T. W., Rackett, C. W., and Nichols, J. A., "Shock Wave Ignition of Magnesium Powders," *Shock Tube and Shock Wave Research, Proceedings of the 11th International Symposium on Shock Tubes and Waves*, edited by B. Ahlborn, A. Hertzberg, and D. Russell, Univ. of Washington Press, Seattle, WA, 1977, pp. 262–268.

[15]Davis, A., "Solid Propellants: The Combustion of Particles of Metal Ingredients," *Combustion and Flame*, Vol. 7, 1963, pp. 359–367.

[16]Nickerson, G. R., Coats, D. E., Dang, A. L., Dunn, S. S., Berker, D. R., Hermsen, R. L., and Lamberty, J. T., "The Solid Propellant Rocket Motor Performance Prediction Computer Program (SPP), Version 6.0," *Engineering Manual*, Vol. 1, U.S. Air Force Astronautics Lab., Rept. AFAL-TR-87-078, 1987.